



HAL
open science

Global socioeconomic exposure of heat extremes under climate change

Jie Chen, Yujie Liu, Tao Pan, Philippe Ciais, Ting Ma, Yanhua Liu, Dai Yamazaki, Quansheng Ge, Josep Peñuelas

► **To cite this version:**

Jie Chen, Yujie Liu, Tao Pan, Philippe Ciais, Ting Ma, et al.. Global socioeconomic exposure of heat extremes under climate change. *Journal of Cleaner Production*, 2020, 277, pp.123275. 10.1016/j.jclepro.2020.123275 . hal-02970803

HAL Id: hal-02970803

<https://hal.science/hal-02970803v1>

Submitted on 7 Jun 2023

HAL is a multi-disciplinary open access archive for the deposit and dissemination of scientific research documents, whether they are published or not. The documents may come from teaching and research institutions in France or abroad, or from public or private research centers.

L'archive ouverte pluridisciplinaire **HAL**, est destinée au dépôt et à la diffusion de documents scientifiques de niveau recherche, publiés ou non, émanant des établissements d'enseignement et de recherche français ou étrangers, des laboratoires publics ou privés.



Distributed under a Creative Commons Attribution - NonCommercial - NoDerivatives 4.0 International License

This is the **accepted version** of the article:

Chen, Jie Chen; Liu, Yujie; Pan, Tao; [et al.]. «Global socioeconomic exposure of heat extremes under climate change». *Journal of cleaner production*, Vol. 277 (Dec. 2020), art. 123275. DOI 10.1016/j.jclepro.2020.123275

This version is available at <https://ddd.uab.cat/record/232214>

under the terms of the  license

2 **Global socioeconomic exposure of heat extremes**

3 **under climate change**

4 Jie Chen^{1,2}, Yujie Liu^{1,2,*}, Tao Pan¹, Philippe Ciais³, Ting Ma⁴, Yanhua Liu¹, Dai
5 Yamazaki⁵, Quansheng Ge^{1,2}, & Josep Peñuelas^{6,7}

6 ¹Key Laboratory of Land Surface Pattern and Simulation, Institute of Geographic Sciences and
7 Natural Resources Research, Chinese Academy of Sciences (CAS), Beijing, China

8 ²University of Chinese Academy of Sciences (UCAS), Beijing, China

9 ³Laboratoire des Sciences du Climat et de l'Environnement, IPSL-LSCE CEA CNRS UVSQ, Gif-
10 sur-Yvette, France

11 ⁴State Key Laboratory of Resources and Environmental Information System, Institute of
12 Geographic Sciences and Natural Resources Research, Chinese Academy of Sciences (CAS),
13 Beijing, China

14 ⁵Institute of Industrial Sciences, University of Tokyo, Tokyo, Japan

15 ⁶CSIC, Global Ecology CREAM-CSIC-UAB, Bellaterra, 08193 Barcelona, Catalonia, Spain

16 ⁷CREAF, Cerdanyola del Vallès, 08193 Barcelona, Catalonia, Spain

17

18 * Corresponding author at: No.11A, Datun Road, Chaoyang District, Beijing, China

19 E-mail address: liuyujie@igsrr.ac.cn (Yujie Liu)

20 **Abstract**

21 Growing evidence indicates that the risk of heat extremes will increase as climate
22 change progresses and create a significant threat to public health and the economy.
23 Socioeconomic exposure is the key component for assessing the risk of such events. To
24 quantify socioeconomic exposure to heat extremes for 2016–2035 and 2046–2065, we
25 use the projections of five global climate models forced by using three representative
26 concentration pathways (RCPs) and projections of population and gross domestic
27 product (GDP), and we take into account the geographic change in the distribution in
28 shared socioeconomic pathways (SSPs). The exposure of the global population for
29 2046–2065 is the greatest under the RCP8.5-SSP3 scenario, up to $1037(\pm 164) \times 10^9$
30 person-days, and the global GDP exposure for 2046–2065 is greatest under the RCP2.6-
31 SSP1 scenario, up to $18(\pm 2) \times 10^{15}$ dollar-days. Asia has the highest exposure among
32 all continents for both population and GDP, accounting for over half of the global
33 exposure. Africa has the largest increase in exposure, with the annual population and
34 GDP exposures increasing by over 9- and 29-fold, respectively, compared with the base
35 period (1986–2005). The effect of climate makes the dominant contribution (47%–53%)
36 globally for the change in population exposure. Changes in the geographic distribution
37 of GDP cause nearly 50% of the total change in GDP exposure for 2016–2035.
38 Mitigating emissions of greenhouse gases, either at the level of the RCP2.6 scenario or
39 at a more ambitious target, is essential for reducing socioeconomic exposure to heat

40 extremes. In addition, designing and implementing effective measures of adaptation are
41 urgently needed in Asia and Africa to aid socioeconomic systems suffering from heat
42 extremes due to climate change.

43 **Keywords** socioeconomic exposure; heat extremes; climate change; population
44 exposure; gross domestic product (GDP) exposure

45 **1 Introduction**

46 Climatic extremes cause extensive economic damage each year, and the risks are
47 expected to increase with continued socioeconomic development and climate change.
48 Risk is usually represented as the probability of occurrence of hazardous events or
49 trends multiplied by the impact if these events or trends occur. Risk is due to the
50 interaction of hazard, exposure, and vulnerability. Exposure usually refers to the people,
51 livelihoods, resources, infrastructure, and economic, social, or cultural assets in places
52 and settings that could be adversely affected (IPCC, 2014). The prediction of changes
53 in exposure to future climatic extremes could, therefore, contribute to the need to
54 consider effective countermeasures to reduce vulnerability and risk. Global
55 socioeconomic exposure (i.e., exposure of the population and gross domestic product,
56 GDP) under climate change has received less attention (Burke et al., 2015; Carleton
57 and Hsiang, 2016), despite recent progress in assessing the hazards of climatic extremes
58 (Hirabayashi et al., 2013; Cook et al., 2014; King et al., 2017; Huang et al., 2017; Nath
59 et al., 2017). Such estimates are urgently needed to clarify future spatiotemporal
60 variation and changes in global socioeconomic exposure and thereby avoid adverse
61 effects on public health and the economy. The importance of assessing exposure is
62 gradually being recognized, as indicated by the published reports of the
63 Intergovernmental Panel on Climate Change (Field et al., 2012; IPCC, 2013), the
64 proposal of a new set of shared socioeconomic pathways (SSPs, O'Neill et al., 2014),
65 and some recent studies of the risk of climate change that considers the effects of
66 socioeconomic factors (Ceola et al., 2015; Mora et al., 2017; Zhang et al., 2018). The
67 integration of climate change with the social economy to estimate future risk, the
68 assessment of the relative importance of different factors, and the quantification of
69 uncertainty would provide a basis for adapting to extreme climate change and reducing
70 the risk of heat extremes.

71 Because of climate change, the frequency and intensity of climatic extremes, such as
72 heat extremes, have increased in recent decades and are likely to continue to increase
73 in the coming decades (IPCC, 2013). Heat extremes have been responsible for
74 significant public health threats and economic losses over the last 100 years. Data for
75 historical damage from the International Disaster Database
76 (https://www.emdat.be/emdat_db/) indicate that heat extremes affected 1.03×10^8
77 people, which includes the deaths of 183495 people, and caused worldwide economic
78 losses of 6.33×10^{10} USD from 1936 to 2019. Serious heat extremes have also occurred
79 more frequently in recent decades, such as those in Europe in 2003, 2018 and 2019
80 (Robine et al., 2008), Australia in 2008 (Vaneckova et al., 2008), Russia in 2010

81 (Trenberth and Fasullo, 2012), and China in 2013 (Sun et al., 2014). Socioeconomic
82 exposure and disaster risks will be magnified in a warmer future (Jones, and O'Neill,
83 2016; Smirnov et al., 2016), when the more frequent and intense heat extremes of this
84 century (Fischer and Knutti 2015; Kharin et al., 2013) combine with a greater
85 population and the accumulation of wealth.

86 In socioeconomic systems, population is most closely related to heat extremes
87 because of its direct impact on public health (Wang et al., 2019). Various economic
88 sectors also can be seriously affected by heat extremes, such as agriculture (water
89 shortages) and industries that rely heavily on hydropower. In addition, tourism,
90 transportation, construction, and other industries are also affected by heat extremes to
91 varying degrees (IPCC, 2014). Considering the data on historical damage of heat
92 extremes (number of people affected, total damage on the economy, etc.) and the
93 availability of simulated socioeconomic data for the future, we selected population and
94 economic activity, expressed as GDP, to determine the impact of heat extremes on the
95 socioeconomic system. Many studies that have quantified future socioeconomic
96 exposure have not considered changes in populations or GDP but assumed that these
97 variables remain constant, which is inappropriate for predicting changes in exposure
98 (Bouwer, 2013; Sun et al., 2017). Most studies have also focused on changes in
99 exposure based on a specific pathway of emission of a greenhouse gas (GHG) or a
100 target of global mean temperature (GMT) rise such as 1.5 °C or 2.0 °C (Harrington and
101 Otto, 2018; Mishra et al., 2017). These analyses of the spatiotemporal variation in
102 exposure between scenarios and time periods are thus insufficient because the
103 population and economy (usually calculated by GDP) are both essential elements in
104 socioeconomic systems and are the factors most severely affected by climatic extremes.
105 The exposures of populations and GDP are usually predicted separately, and these two
106 elements are rarely used to assess socioeconomic exposure (Bowles et al., 2014;
107 Forzieri et al., 2017), although the spatial distributions of populations and economies
108 are also consistent. Given these factors, we focus in this work on simulating the global
109 exposure to extreme heat as a function of changes in climate and population or GDP.
110 The results constitute a first step toward understanding how interactions between
111 climate change and socioeconomic systems affect exposure patterns.

112 This study systematically quantify the global spatiotemporal distribution of and
113 changes in exposure of population and GDP to heat extremes under different scenarios
114 and over different time periods. Bias-corrected projections of five global climate
115 models (GCMs, Table 1) driven by representative concentration pathways (RCPs) are
116 used to calculate the frequency of extreme heat events (see Sec. 2.1, Materials).
117 Combined with population and GDP projections in SSPs (Figs. S1 and S2), which
118 consider changes in the geographic distribution of population and GDP (see Sec. 2.1,
119 Materials), the spatiotemporal variation of global exposure to extreme heat of the
120 population and GDP is quantified in both the base period (1986–2005) and in future
121 periods (2016–2035 and 2046–2065) under various scenarios (see Sec. 2, Materials and
122 Methods). We also assess the relative importance of climatic and socioeconomic factors
123 and their uncertainties to characterize the contribution of climate change and growth in
124 population and GDP to future changes in extreme-heat exposure. The main target of

125 this study is quantifying the impact of heat extremes on socioeconomic system under
126 climate change to characterize variation of socioeconomic exposure among scenarios
127 and periods, distinguish high exposure regions, and identify dominant contributor for
128 exposure change, so as to support policymakers in the development of climate change
129 mitigation and adaptation strategies.

130 **2 Materials and Methods**

131 **2.1 Materials**

132 Daily climatic data were obtained from the Inter-Sectoral Impact Model
133 Intercomparison Project (ISI-MIP, Warszawski et al., 2014) for the Coupled Model
134 Intercomparison Project Phase 5 (CMIP5, Taylor et al., 2012) (Table 1), which contains
135 simulations from five GCMs based on RCPs. The RCP scenarios represent pathways
136 based on simulated impacts on land use, aerosol emissions, and GHGs (Vuuren et al.,
137 2011). The four RCPs cover the period up to 2100 and have radiative forcings from the
138 open literature that vary from 2.6 to 8.5 W/m². The scenarios, RCP2.6, RCP4.5, and
139 RCP8.5, which represent low, middle, and high GHG emissions, respectively, were
140 selected for analysis (Vuuren et al., 2011). RCP6.0, which is interpreted as either a
141 medium baseline or a high-mitigation case between RCP4.5 and RCP8.5, is not used.
142 The base period was 1986–2005, which is the commonly used reference period in
143 assessments of projected changes in extreme indices and climate impacts (Schleussner
144 et al., 2016). Future periods in the 2030s and 2050s were given lengths of 20 years
145 (2016–2035 and 2045–2065) to be consistent with the base period. The spatial
146 resolution of the output data was offset-corrected and converted to 0.5° × 0.5° latitude
147 and longitude by spatial downscaling. Statistical bias-correction methods facilitate the
148 comparison between observed and simulated data during the historical reference period
149 and for a continuous transition into the future (Hempel et al., 2013). Preservation of
150 absolute changes in monthly temperature and relative changes in monthly precipitation
151 in each grid cell implies that the global warming trend and the climate sensitivities of
152 the GCMs are preserved, and the trend and the long-term mean are well represented,
153 which ensures the credibility of the simulated data (Hempel et al., 2013; Warszawski et
154 al., 2014).

155 The United Nations, the World Bank, and other organizations proposed future
156 socioeconomic projections for population and GDP. Many previous studies also
157 combined current socioeconomic data with future climatic data for analysis, although
158 these studies neglected to consider how changes in socioeconomic factors affect
159 exposure. We used the predictions of population and GDP from the scenarios of SSPs
160 based on the selected RCP scenarios. SSPs are reference pathways describing possible
161 alternative trends in the evolution of societies and ecosystems on a timescale of 100
162 years without climate change or implementation of climate policies (Riahi et al., 2017).
163 RCP2.6, 4.5, and 8.5 generally correspond to SSP1, 2, and 3, respectively, based on the
164 correspondence between the RCPs and SSPs provided by the IPCC (O'Neill et al., 2014,
165 Table S4). We therefore selected SSP1, 2, and 3 for this study. The RCP2.6-SSP1

166 scenario assumes low carbon emissions, sustainable development proceeding at a
 167 reasonably high pace, and fewer inequalities. The RCP4.5-SSP2 scenario assumes
 168 moderate carbon emissions with medium growth in population and GDP. Finally, the
 169 RCP8.5-SSP3 scenario assumes high carbon emissions with a rapidly growing
 170 population and a low adaptive capacity. The projections of population and GDP were
 171 obtained from the National Institute for Environmental Studies, Japan (NIES), which
 172 were downscaled from the International Institute for Applied Systems Analysis
 173 (IIASA). The spatial resolution was also $0.5^\circ \times 0.5^\circ$ latitude and longitude. The
 174 population and GDP projections were downscaled with explicitly considered spatial
 175 and socioeconomic interactions between cities, and they used auxiliary variables,
 176 including road network and land cover. The downscaling results were consistent with
 177 the scenario assumptions and captured the difference in urban and non-urban areas in a
 178 more reasonable manner, which ensures the prediction accuracy of the SSPs (Murakami
 179 and Yamagata, 2016).

180 Table 1. Description of global climate models (GCMs).

Model	Institute	Atmospheric resolution (longitude \times latitude)
GFDL-ESM2M	Geophysical Fluid Dynamics Laboratory	$2.5^\circ \times 2^\circ$
HadGEM2-ES	National Institute of Meteorological Research/Korea Meteorological Administration	$1.875^\circ \times 1.25^\circ$
IPSL-CM5A-LR	Institute Pierre-Simon Laplace	$3.75^\circ \times 1.875^\circ$
MIROC-ESM- CHEM	Japan Agency for Marine-Earth Science and Technology, Atmosphere and Ocean Research Institute (University of Tokyo), and National Institute for Environmental Studies	$2.8^\circ \times 2.8^\circ$
NorESM1-M	Norwegian Climate Centre	$2.5^\circ \times 1.89^\circ$

181

182 2.2 Methods

183 2.2.1 Hazards of extreme heat

184 Annual days of extreme heat, which is also the frequency of extreme heat, were
 185 used to quantify the hazard, which is defined as the daily maximum temperature
 186 exceeding a threshold. The threshold for extreme heat was defined as the 90th percentile
 187 of daily maximum temperatures for the base period (1986–2005) and was set at 25°C
 188 when the local 90th percentile was $<25^\circ\text{C}$ (Garssen et al., 2005). We chose relative
 189 thresholds rather than a fixed threshold to project global spatiotemporal variation and
 190 changes in exposure because no single fixed threshold suffices for the substantial
 191 differences in climatic conditions around the world (Gasparri et al., 2015). Relative
 192 thresholds were, therefore, the simplest definitions of regionally relevant extreme heat
 193 around the globe. The frequency of extreme heat was calculated as follows:

$$C = \sum_{i=1}^{365} (TEM_i > THR), \quad (1)$$

$$\bar{C} = \frac{\sum_{j=1}^5 C_j}{5}, \quad (2)$$

194 where C is the annual number of days of extreme heat (day), i is the i^{th} day of a year,
 195 TEM is the daily maximum temperature ($^{\circ}\text{C}$), THR is the local threshold ($^{\circ}\text{C}$), \bar{C} is the
 196 multi-model averaged value of C (day), and j is the j^{th} GCM.

197 2.2.2 Exposure to extreme heat

198 We measured population and GDP exposure for each grid cell as the number of
 199 extreme heat days multiplied by the number of people and GDP, respectively (Jones et
 200 al., 2015). Therefore, the units of population and GDP exposures are person-days and
 201 purchasing power parity (PPP) dollar-days, respectively. To calculate exposure in the
 202 base period and in the future periods (2016–2035 and 2046–2065), we minimized
 203 interannual variations by using 20-year averages of annual extreme heat days and of the
 204 projections of population and GDP. The 20-year mean exposure for each projection of
 205 the five climate models was calculated for the base period and for the future periods.
 206 Moreover, exposure for the grid cells was also aggregated to global and continental
 207 scales for further analysis. Explicitly, we have

$$\overline{E_P} = \frac{\sum_{m=1}^{20} C_m \times P}{20}, \quad (3)$$

$$\overline{E_G} = \frac{\sum_{m=1}^{20} C_m \times G}{20}, \quad (4)$$

208 where $\overline{E_P}$ is the 20-year-averaged population exposure (person-day), m is the m^{th} year
 209 of the study period, C is the number of annual days of extreme heat (day), P is the
 210 simulated population number (person), $\overline{E_G}$ is the 20-year-averaged GDP exposure
 211 (PPP \$-day), and G is the GDP simulation (PPP \$).

212 2.2.3 Analysis of relative importance of change in exposure and cumulative 213 probability

214 Using techniques from a previous study (Jones et al., 2015), we evaluated the relative
 215 importance of the effects of different factors by categorizing the changes in population
 216 and GDP exposures in terms of the effects of climate, population, GDP, and interactions.
 217 The impact of population and GDP was calculated by holding climate constant (i.e., the
 218 20 year averages of annual days of extreme heat for the base period were multiplied by
 219 the populations and GDPs in the RCP-SSP scenarios). Population and GDP were
 220 similarly held constant when calculating the impact of climate (i.e., the population for
 221 the base period was multiplied by the 20 year averages of annual days of extreme heat
 222 in the RCP scenarios). The interactive effect was also calculated to determine whether
 223 the areas with continued population and GDP growth experienced more heat extremes
 224 under climate change. The changes in population and GDP exposure were categorized

225 as follows:

$$\Delta E_P = C_b \Delta P + P_b \Delta C + \Delta P \Delta C, \quad (5)$$

226

$$\Delta E_G = C_b \Delta G + G_b \Delta C + \Delta G \Delta C, \quad (6)$$

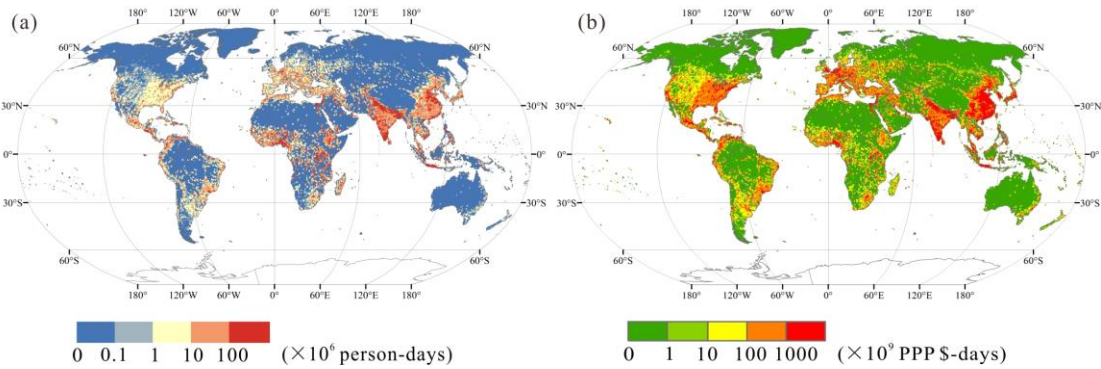
227 where ΔE_P is the total change in population exposure, ΔE_G is the total change in GDP
228 exposure, C_b is the annual days of extreme heat for the base period, P_b and G_b are
229 the population and GDP for the base period, respectively, ΔC is the change in annual
230 days of extreme heat from the base period to future periods, and ΔP and ΔG are the
231 changes in population and GDP, respectively, from the base period to future periods.
232 Therefore, $C_b \Delta P$ is the population effect, $C_b \Delta G$ is the GDP effect, $P_b \Delta C$ and
233 $G_b \Delta C$ are the climatic effects, and $\Delta P \Delta C$ and $\Delta G \Delta C$ are the interactive effects.

234 The uncertainties of changes in population and GDP exposure for future scenarios
235 were analyzed to evaluate the possible impact of climate change and growth on
236 population and GDP. The probability analysis of changes in population and GDP were
237 first separately calculated in each GCM based on the cumulative distribution function
238 (CDF). Next, the mean value and standard deviation for the five GCMs were computed.
239 The CDF of a random variable X represents the probability that $X \leq x$.

240 3 Results

241 3.1 Spatial pattern of population and GDP exposures to extreme heat

242 Figure 1 shows the multi-model average exposures of the population and GDP for
243 RCP8.5-SSP3 for 2046–2065. Figure S3 shows the frequency of extreme heat, and Figs.
244 S4 and S5 show the population and GDP exposures, respectively. Tables S1 and S2
245 present the statistics for population and GDP exposures globally and continentally for
246 the RCP-SSP scenarios and the different time periods.



247

248 Fig. 1: Multi-model global projections of average exposures of (a) population and (b)
249 GDP to extreme heat for the RCP8.5-SSP3 scenario for 2046–2065. PPP is purchasing
250 power parity in USD.

251 The spatial distribution of the frequency of heat extremes indicates latitudinal
252 zonality in each time period and for each scenario (Fig. S3). The threshold in the base
253 period exceeds 25 °C, except at latitudes >50° and on the Qinghai-Tibet Plateau. Heat
254 extremes are most frequent near the equator, and their frequency gradually decreased
255 with increasing latitude in both the base period and future periods. The frequency of

256 extreme heat clearly increases over time. The highest frequency is 36.5 days in the base
257 period, whereas the frequency is projected to exceed 120 days in the RCP scenarios.
258 The frequency is significantly higher for 2046–2065 than 2016–2035 under each
259 scenario. The frequency is highest under the RCP8.5 scenario and lowest under RCP2.6,
260 but the difference between the scenarios is less than the difference between the time
261 periods.

262 The regions with high population and GDP exposures to extreme heat are primarily
263 concentrated in densely populated areas, such as India, China, midwestern Europe, the
264 eastern USA, and the coastal areas of South America, for both the base period and the
265 projected scenarios (Fig. 1). Exposure is also high near the equator in Africa because
266 of the frequent occurrence of extreme heat. Population exposure under the RCP
267 scenarios is highest for India and the east coast of China ($>10 \times 10^6$ person-days). GDP
268 exposure is much higher for eastern China, the Indian subcontinent, western Europe,
269 and eastern North America than other locations such as northern Asia, northern North
270 America, and Middle Oceania, with annual GDP exposure $>100 \times 10^9$ PPP dollar-days.

271 **3.2 Global and continental change in exposure to extreme heat**

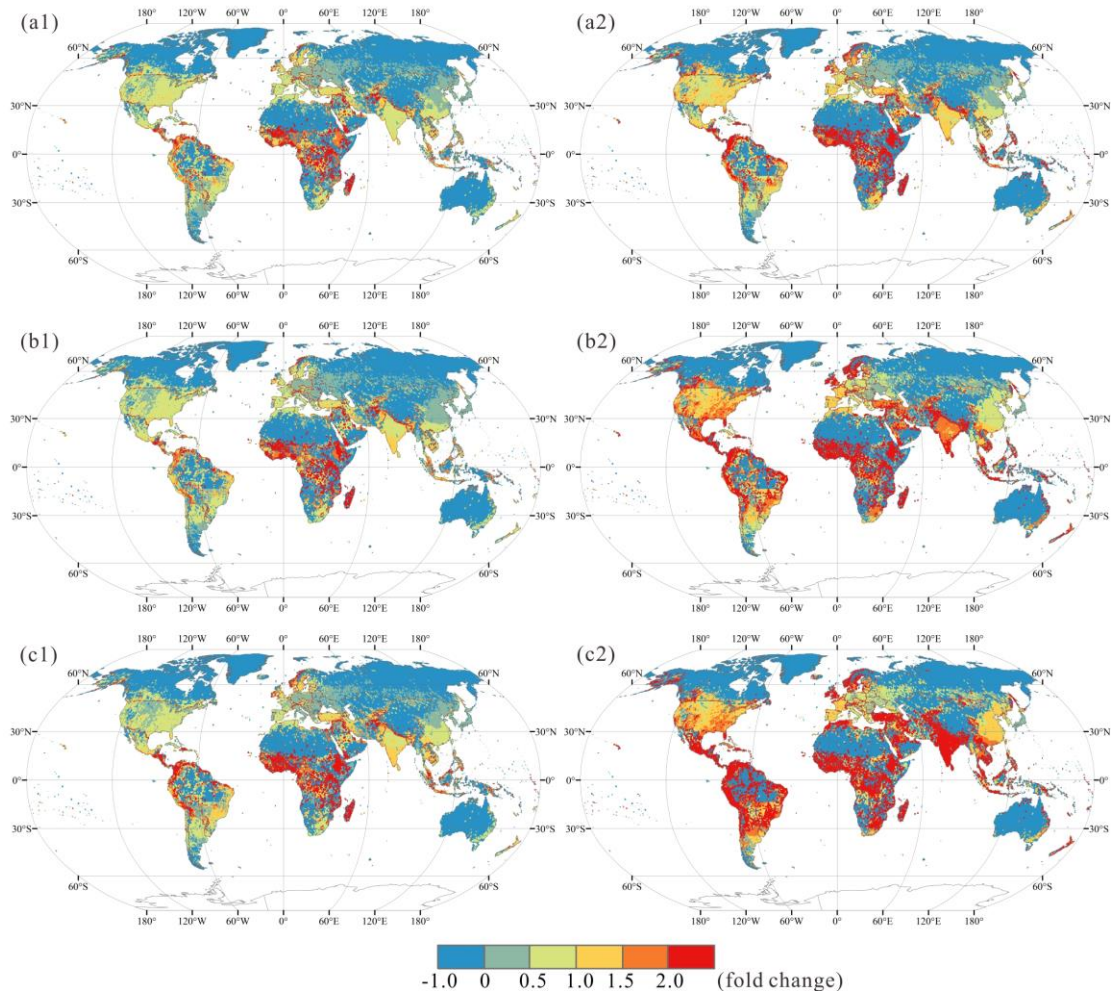
272 Annual exposure of the global population for the base period is 217.80×10^9 person-
273 days, which increases to 1037.06×10^9 person-days for 2046–2065 under the RCP8.5-
274 SSP3 scenario (Table S1). The increase in population exposure is largest for the
275 RCP8.5-SSP3 scenario and smallest for RCP2.6-SSP1 (Fig. 2). The increase in global
276 annual GDP exposure is largest for 2046–2065 under the RCP2.6-SSP1 scenario (Fig.
277 3), with a 10.47-fold increase in exposure relative to the base period (Table S2). In
278 contrast, the increase is smallest for 2016–2035 under RCP8.5-SSP3, with an increase
279 of only 3.71-fold relative to the base period. The reason that the highest GDP exposure
280 appears in the RCP2.6-SSP1 scenario is that SSP1 is a “sustainable” scenario that
281 assumes economic growth is shared at the global scale, so GDP increases relatively
282 more in countries that currently have less wealth. Therefore, the exposed GDP at the
283 global scale is higher in RCP2.6-SSP1, despite the hazard of extreme heat being lower
284 in RCP2.6.

285 The population exposure is highest for Asia, followed by Africa, and lowest in
286 Oceania in both the base period and the RCP scenarios. Exposure in Asia and Africa in
287 the base period is 63% and 14%, respectively (Table S1). The percentage of population
288 exposure under the three RCP scenarios decreases for Asia and increases for Africa.
289 The percentage of population exposure for 2046–2065 under the RCP8.5-SSP3
290 scenario decreases for Asia to 53% and increases for Africa to 29% of global exposure.
291 Exposure for the continental GDP in the base period ranks as follows: Asia > North
292 America > Europe > South America > Africa > Oceania (Table S2).

293 The percent of GDP exposure increases for Asia, Africa, and South America and
294 decreases for North America, Europe, and Oceania. The increase in both continental
295 population and GDP exposures is largest for Africa, with the annual population
296 exposure >9.20 -fold higher under the RCP8.5-SSP3 scenario for 2046–2065 than for
297 the base period, and the change of population exposure is 1.22-fold larger over the same
298 period and under the same scenarios for Europe than in the base period, which is the

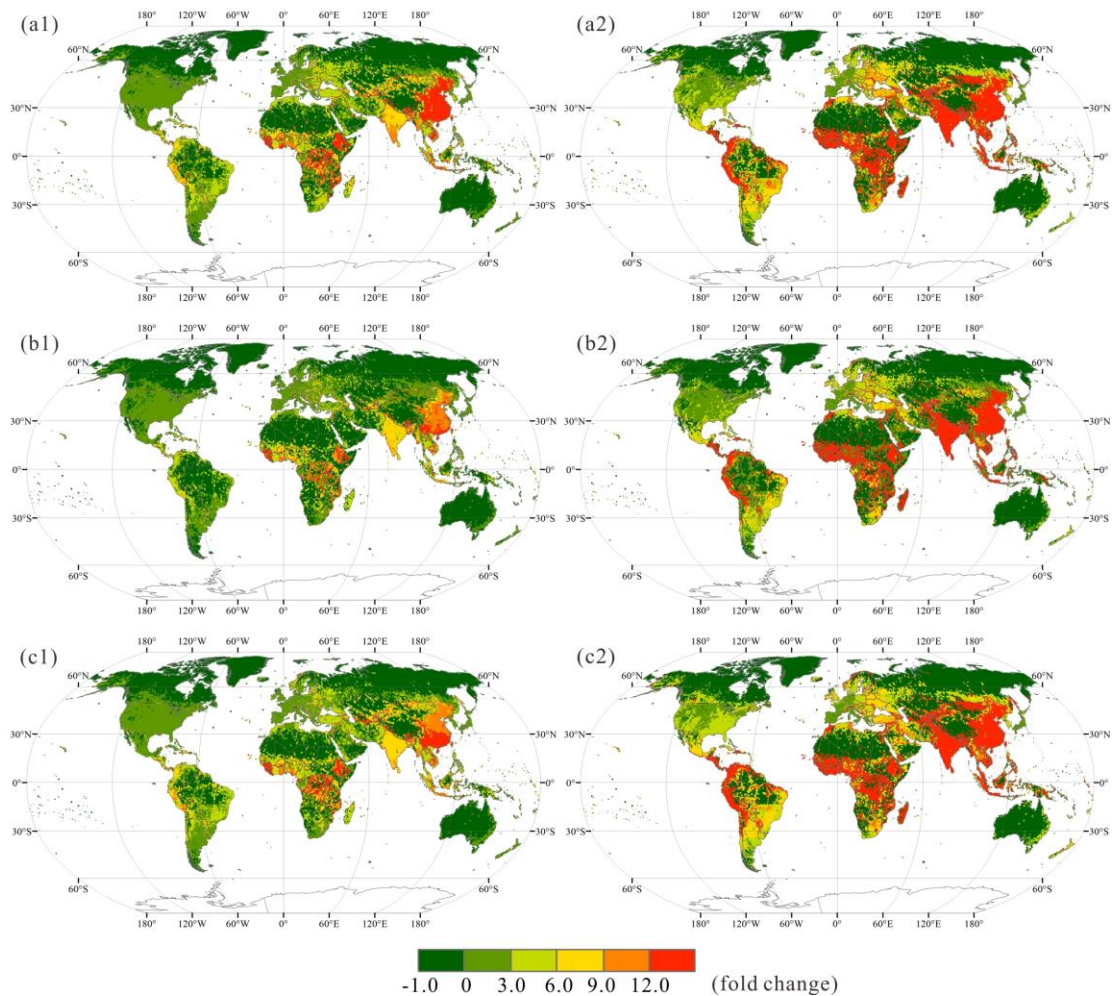
299 smallest change among the continents. GDP exposure increases the most in Africa,
 300 by >29.34-fold relative to the base period under the RCP2.6-SSP1 scenario for 2046–
 301 2065, whereas GDP exposure in North America is 3.99-fold higher for 2046–2065 than
 302 the base period, which is the lowest among continents.

303 Figure 2 presents the relative changes in population exposure for the projected
 304 scenarios relative to the base period. The rate of change is highest in Africa in regions
 305 near the equator. Population exposure for 2016–2035 under the RCP2.6-SSP1 scenario
 306 increases more than 2-fold. The increase in the coastal regions of South America is also
 307 rapid, by more than 2-fold for 2046–2065 under the RCP4.5-SSP2 scenario. The rate
 308 of change, however, is <50% in areas where the rate has usually been high, such as
 309 China, the USA, and Western Europe. Population exposure is much higher for 2046–
 310 2065 than 2016–2035 under each scenario when the differences are compared between
 311 different time periods, with time, the population increases gradually, and when that
 312 increase is crossed with the more frequent heat extremes affected by climate change.
 313 Population exposure is highest under the RC8.5-SSP3 scenario, where population
 314 growth is rapid, followed by the RCP4.5-SSP2 and RCP2.6-SSP1 scenarios.



315
 316 Fig. 2: Multi-model global projections of average relative change in population
 317 exposure to extreme heat for the three RCP scenarios and two time periods relative to
 318 the base period: (a) RCP2.6-SSP1, (b) RCP4.5-SSP2, (c) RCP8.5-SSP3, (1) 2016–2035,
 319 (2) 2046–2065.

320 Figure 3 presents the spatial distributions of the average relative changes in GDP
 321 exposure for the RCP scenarios projected by multiple models. GDP exposure for 2016–
 322 2035 increases most rapidly in eastern China, with a more than 9-fold increase relative
 323 to the base period. GDP exposure also changes for central Africa and the South Asian
 324 subcontinent, with more than 6-fold increases relative to the base period. GDP exposure
 325 increases for 2046–2065 relative to the base period and 2016–2035. The increase in
 326 exposure is largest for Asia and is >12-fold higher than the base period in many
 327 countries, such as China, India, and Mongolia. GDP exposure also changes for Africa,
 328 South America, and Eastern Europe. The change in exposure is relatively small for
 329 North America and Oceania, less than 6-fold relative to the base period. GDP exposure
 330 is highest under the RC2.6-SSP1 scenario, where GDP growth is fastest, followed by
 331 the RCP4.5-SSP2 and RCP8.5-SSP3 scenarios.



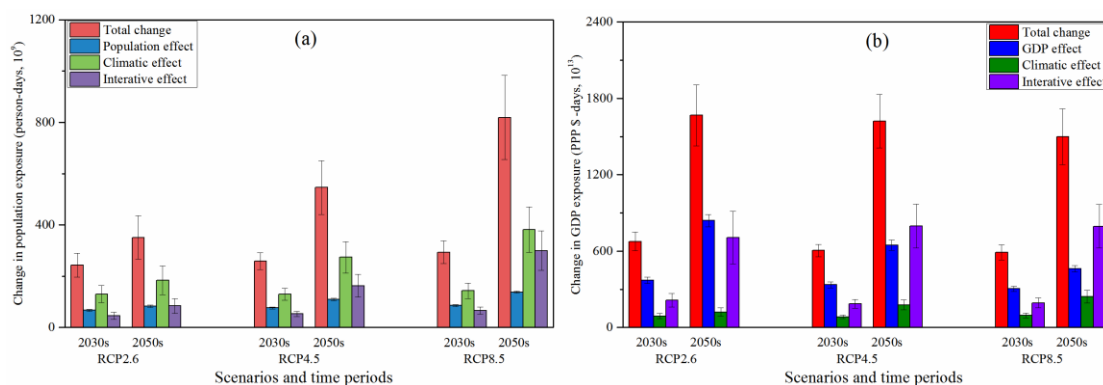
332
 333 Fig. 3: Multi-model global projections of average relative change in GDP exposure to
 334 extreme heat for the three RCP scenarios and two time periods relative to the base
 335 period: (a) RCP2.6-SSP1, (b) RCP4.5-SSP2, (c) RCP8.5-SSP3, (1) 2016–2035, (2)
 336 2046–2065.

337 3.3 Analysis of relative importance of change in exposure

338 To determine the relative importance of various factors, we categorize the changes
 339 in population and GDP exposures in terms of the effects of population, GDP, climate,

340 and their interactions. Figures 4–6 show the changes in exposure and its components
 341 for the globe and for the continents under the three RCP scenarios. The change in global
 342 exposure of the population is primarily affected by the climate, whereas the change in
 343 global exposure of GDP is mainly attributed to the GDP effect (Fig. 4).

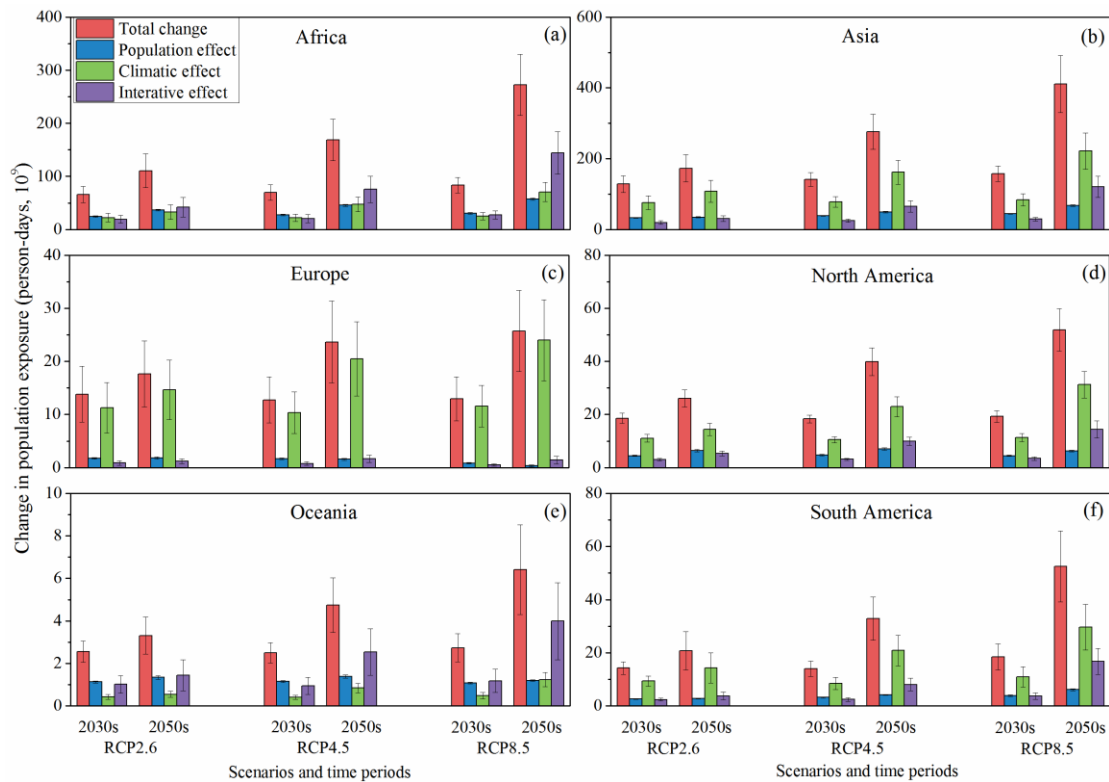
344 The climate effect accounts for nearly half of the total change in population exposure
 345 (47%–53%) in each scenario and for each period. The effect of population change for
 346 2016–2035 is larger than the interactive effect, which reverses for 2046–2065. The GDP
 347 effect is responsible for nearly 50% of the total change in GDP exposure for 2016–2035,
 348 with approximately 30% and 20% attributable to the effects of climate and interactions,
 349 respectively. The change in GDP exposure for 2046–2065 under the RCP4.5-SSP2 and
 350 RCP8.5-SSP3 scenarios is dominated by the interactive effect, at 49% and 53%,
 351 respectively, followed by the effects of GDP and climate. The increase in the influence
 352 of the interactive effect highlights the importance of the interactions between GDP and
 353 climate change in increasing GDP exposure under the scenarios of high GHG emissions.



354

355 Fig. 4: Categorization of projected aggregate global changes in (a) population and (b)
 356 GDP exposure to extreme heat under the RCP2.6-SSP1, RCP4.5-SSP2, and RCP8.5-
 357 SSP3 scenarios. Error bars are the standard deviations for the results of the five GCMs.
 358 PPP is purchasing power parity in USD.

359 The relative importance of the factors of change in population exposure at the
 360 continental level varies between regions (Fig. 5). As noted above, the percent of
 361 population exposure worldwide is highest for Asia and Africa, but the dominant
 362 contribution to the change differs between the two continents. The effect of climate is
 363 the dominant contribution for Asia, Europe, North America, and South America for all
 364 scenarios and periods. This result indicates that an increased frequency of heat extremes
 365 amplifies population exposure, even in the absence of population increases on these
 366 continents. In contrast, the contribution of the three factors (i.e., the effects of
 367 population, climate, and the interaction) for Africa is nearly identical for 2016–2035
 368 because of the strong population increase projected for this continent. The interactive
 369 effect, however, becomes the primary contribution for 2046–2065, particularly under
 370 the RCP8.5-SSP3 scenario, accounting for 53% of the total change, which is more than
 371 the sum of the population and interactive effects. The contributions of the GDP and
 372 interactive effects for Oceania are nearly the same for 2016–2035 under the three
 373 scenarios. In contrast, the interactive effect makes the primary contribution to the
 374 change in GDP exposure for 2046–2065 under the RCP4.5-SSP2 and RCP8.5-SSP3

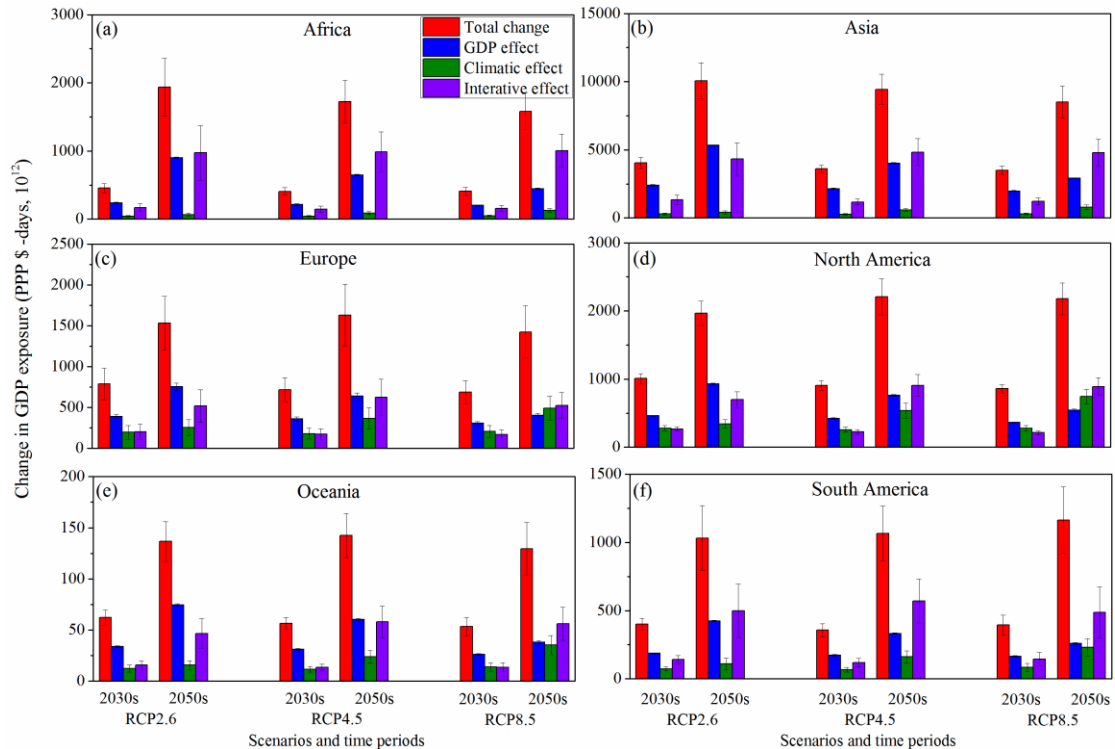


376

377 Fig. 5: Categorization of projected aggregate continental change in population exposure
 378 to extreme heat under the RCP2.6-SSP1, RCP4.5-SSP2, and RCP8.5-SSP3 scenarios.
 379 Error bars are the standard deviations for the results of the five GCMs: (a) Africa,
 380 Asia, (c) Europe, (d) North America, (e) Oceania, (f) South America.

381 Between continents, the differences in relative importance to GDP exposure to the
 382 effects of GDP, climate, and interactions are clear (Fig. 6), and the contribution of GDP,
 383 climatic, and interactive effects under the various scenarios and periods also varies
 384 among continents. The largest contribution for Asia and North America is from GDP
 385 for 2016–2035 under the three scenarios and for 2046–2065 under the RCP2.6-SSP1
 386 scenario, whereas the interactive effect is the dominant contribution for 2046–2065
 387 under the RCP4.5-SSP2 and RCP8.5-SSP3 scenarios. The GDP effect for Africa and
 388 South America is the primary contributor for 2016–2035, whereas the interactive effect
 389 is the primary contributor for 2046–2065. The difference between the interactive and
 390 GDP effects also increases for the pathways involving high GHG emissions in these
 391 two continents. The interactive effect for the RCP8.5-SSP3 scenario accounts for 64%
 392 of the total change for Africa, exceeding the contribution of 35% for the GDP effect.
 393 The interactive effect accounts for 58% of the total change for South America, whereas
 394 the GDP effect accounts for only 22%. The increase in GHG emissions leading to
 395 climate change and more frequent heat extremes can account for the increase in the
 396 difference between the interactive and GDP effects. The interaction between climate
 397 and change in GDP amplifies the exposure, but the GDP effect decreases, and the
 398 interactive effect increases as GDP growth slows under the pathways with high GHG
 399 emissions, which leads to the large difference between the effects under the RCP8.5-
 400 SSP3 scenario. The GDP effect is the primary contributor for Europe and Oceania for

401 all periods and scenarios, except for 2046–2065 under the RCP8.5-SSP3 scenario,
 402 which implies that GDP exposure on these two continents would increase quickly
 403 without the impact of climate change. For almost all continents, GDP exposure is
 404 dominated by the GDP effect under the RCP2.6-SSP1 scenario because GDP grows
 405 fastest under this scenario.



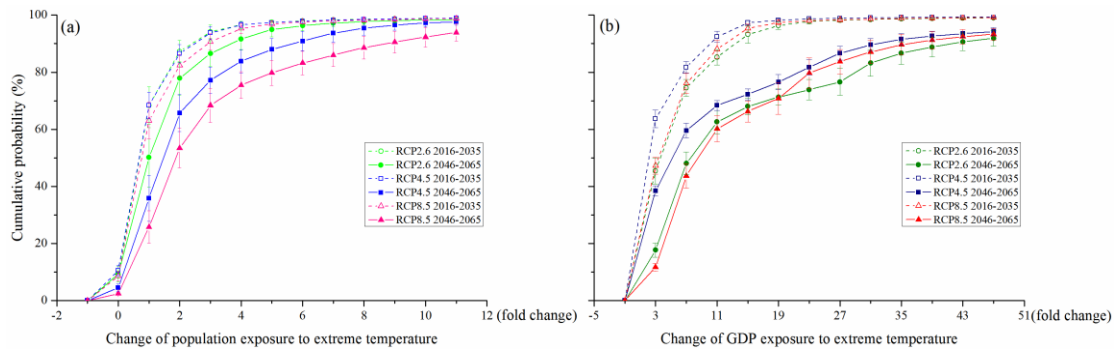
406

407 Fig. 6: Categorization of projected aggregate continental change in GDP exposure to
 408 extreme heat under the RCP2.6-SSP1, RCP4.5-SSP2, and RCP8.5-SSP3 scenarios.
 409 Error bars are the standard deviations for the results of the five GCMs. PPP is
 410 purchasing power parity in USD: (a) Africa, (b) Asia, (c) Europe, (d) North America,
 411 (e), Oceania, (f) South America.

412 3.4 Analysis of cumulative probability of changes in population and GDP 413 exposures

414 Figure 7 shows the cumulative distribution functions for changes in population and
 415 GDP exposures under the various scenarios and time periods relative to the base period.
 416 The changes are smaller for 2016–2035 than 2046–2065 for both population and GDP
 417 exposure, which indicates that population and GDP exposures increase rapidly over
 418 time, independent of the scenario. Population and GDP exposures, however, differ
 419 between the three scenarios and the two time periods. The cumulative probability of an
 420 increase in population exposure is >90% for 2016–2035 and >95% for 2046–2065. The
 421 change is largest under RCP8.5-SSP3, with 90% probability of a zero- to 10-fold
 422 increase for both periods, followed by RCP4.5-SSP2 and RCP2.6-SSP1, with a 90%
 423 probability of a zero- to 7-fold increase relative to the base period. The future increase
 424 is much faster for GDP exposure than for population exposure because of the faster
 425 growth in GDP. The change in GDP exposure for 2046–2065 under the RCP2.6-SSP1

426 scenario is the largest among all time periods and scenarios, with 90% probability of a
 427 difference of -1- to 43-fold, with a 10% probability for an increase >43-fold relative to
 428 the base period. The increase for 2046–2065 is -1- to 35-fold under RCP8.5-SSP3 and
 429 -1- to 31-fold under RCP4.5-SSP2 for the same probability. The changes are much
 430 smaller for 2016–2035 than for 2046–2065, with >70% probability of a zero- to 7-fold
 431 increase for the three scenarios. The change for 2046–2065 is largest under RCP2.6-
 432 SSP1, with nearly a 15% probability of a >15-fold increase relative to the base period,
 433 whereas the increases are 7- and 11-fold under the RCP4.5-SSP2 and RCP8.5-SSP3
 434 scenarios, respectively, for the same probability.



435

436 Fig. 7: Cumulative probability of projected change in (a) population exposure and (b)
 437 GDP exposure to extreme heat relative to the base period. Error bars are the standard
 438 deviations for the results of the five GCMs.

439 4 Discussion

440 4.1 Impact of a warmer climate on socioeconomic exposure to extreme heat

441 Our study shows spatiotemporal variation and changes in exposure and its
 442 components at global and continental levels. The results indicate variations among the
 443 continents (Figs. S4 and S5). For example, population exposure is highest in Asia (Fig.
 444 S4), accounting for >50% of the global exposure, followed by Africa, North America,
 445 Europe, South America, and Oceania. The percent of population exposure for Africa
 446 and South America is projected to increase over time and with an increase in GHG
 447 emissions, whereas the percentage of population exposure for Asia, Europe, and North
 448 America is projected to decrease over time. GDP exposure accounted for >50% of the
 449 total exposure for Asia (Fig. S5), with likely increases under the future scenarios,
 450 followed by North America, Europe, Africa, South America, and Oceania. The percent
 451 of exposure for developing countries, such as in Africa and South America, increases
 452 for the future scenarios. In contrast, decreases would be likely for developed countries,
 453 such as those in North America, Europe, and Oceania. Extreme heat under climate
 454 change would thus affect Asia the most, where population and GDP exposures are
 455 highest. Exposure for Africa is expected to increase rapidly in the future. Therefore,
 456 more attention should be directed to Asia and Africa for deeper research on extreme
 457 heat exposure and risk assessment. In addition, the design and implementation of
 458 effective adaptive measures are urgently needed in regions with high socioeconomic

459 exposure, to lessen populations suffering from heat extremes and reduce the economic
460 losses under climate change.

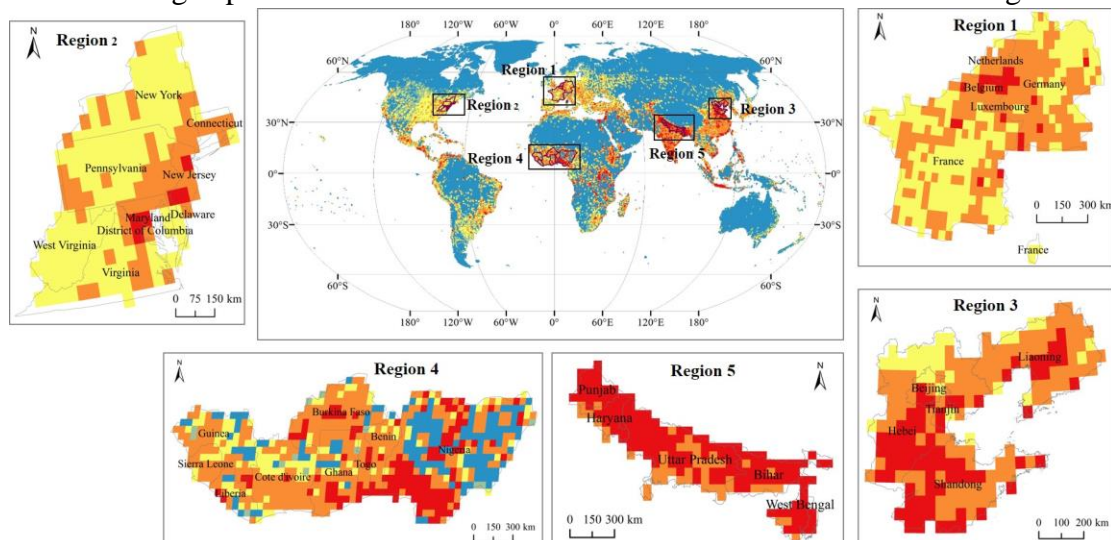
461 We estimate future socioeconomic exposure based on SSP projections with to various
462 RCP scenarios. Because the current data are well understood and widely accepted,
463 however, some previous research is based on current spatial distributions and
464 population and GDP exposures (Hsiang et al., 2017). We also calculate exposure to
465 future extreme heat regardless of changes in population and GDP (Table S3). The
466 results indicate that socioeconomic exposure would increase significantly under climate
467 change, with distinct differences among the RCP scenarios, even if population and GDP
468 exposures are maintained at current levels. Exposure is lowest under the RCP2.6
469 scenario and highest under the RCP8.5 scenario. Population and GDP exposures are
470 1.72- and 1.67-fold higher under RCP8.5 than under RCP2.6, respectively. Both results
471 for the SSP projections and the current fixed values highlight the importance of
472 reducing emissions. Overall, it is potential to mitigate the impact of climate change on
473 both extreme heat hazards and population exposures under the RCP2.6 scenario
474 compared to RCP4.5 and 8.5 scenarios. And the efficiency of reducing emissions
475 should be further quantified in future studies under RCP2.6 or other ambitious warming
476 target, such as 1.5°C and 2°C warming target proposed in Paris Agreement (UNFCCC,
477 2015), which will be helpful for making climate change mitigation strategies.

478 **4.2 Uncertainty, limitation and further research**

479 Heat extremes could be measured by using different thresholds (e.g., 90, 95, 97.5,
480 and 99th percentile of daily maximum temperatures over the base period). The spatial
481 patterns of exposure and change are generally similar, whereas the quantity of exposure
482 and the relative importance of factors differ greatly (Liu et al., 2017). Assessing
483 socioeconomic exposure under climate change has many uncertainties, except for the
484 indices that measure extreme heat. The primary sources of uncertainty include scenarios
485 of GHG emission (Maurer, 2007), GCMs (Soden et al., 2018), predictions of population
486 and GDP (Chen et al., 2018) and the calculation method of exposure (Zhang et al.,
487 2018). The research of Bonan and Doney (2018) on global change in stresses on
488 terrestrial and marine ecosystems show that the uncertainty on land is mostly from
489 model uncertainty, which contributes nearly 80% of the total uncertainty in the 21st
490 century. We evaluate population and GDP exposures based on five GCM simulations
491 after downscaling and assessing the various scenarios and time periods separately.
492 Figures 4–7 show the differences between the GCMs. In addition to displaying the mean
493 value of five GCMs, the standard deviation of five GCMs is also displayed as error bars
494 in the figures. This study generates assessments by considering different sources of
495 uncertainty, so the results can be considered as reasonable with relatively high accuracy.

496 This study is also subject to some limitations. First, our study quantified
497 spatiotemporal variation of population and GDP exposures to extreme heat as an
498 important first step for estimating changes in risk, which made progress compared to
499 the previous studies ignoring the spatiotemporal variation of the socioeconomic risk
500 (Barnett et al., 2012; Gasparri and Armstrong, 2011; Voorhees et al., 2011). However,
501 we do not estimate changes in vulnerability due to the lack of more advanced damage

502 data due to heat extremes. In further studies, we should also concentrate on assessing
 503 vulnerability when the data are available, which is also essential for assessing risk. In
 504 addition, adopting measures such as the use of air conditioning and the purchase of
 505 insurance should be taken into account. These factors would likely improve resilience
 506 to heat extremes and thus decrease vulnerability and limit the impact of climate change.
 507 Second, the effect of urban heat islands (UHIs) in addition to global warming is not
 508 considered explicitly in the climate change simulations in this study. UHIs are
 509 confirmed to exacerbate the extent and intensity of heat extremes in urban areas and
 510 increase the risk to urban residents in heat extremes (Dan and Bou-Zeid, 2013; Hajat
 511 and Kosatky, 2010; Mishra et al., 2015). Recently, as the importance of urbanization in
 512 climate change has come to be realized, several case studies simulating the impact of
 513 urbanization on extreme temperature events been done (Chen and Frauenfeld, 2016;
 514 Grossman-Clarke et al., 2010; Wang et al., 2012). Some research focused on intensely
 515 urbanized places such as eastern China, the eastern USA, and Western Europe, which
 516 is consistent with the results of our studies on high-exposure regions. However, some
 517 other regions such as western Africa and northern India are also expected to suffer high
 518 exposure to heat extremes in the future. More attention should be focused on these
 519 regions in future studies (see Fig. 8). However, global studies are rare because of a lack
 520 of precise land-use and population data. Some other studies assess the future urban
 521 climate change by using GCM (Fischer et al., 2012; Oleson, 2012). However, given the
 522 coarse spatial resolution, the influence of GCM on underlying urban surfaces could not
 523 be fully appreciated, so the impact of future urban development on UHIs was not
 524 considered in these studies. As a result, the effect of UHIs on extreme temperature
 525 events may be underestimated. Therefore, in future studies, the design and nesting of
 526 urban land surface models and the estimation of UHI, especially the heat island
 527 estimation during heat extremes, should be taken into account, since they are critical
 528 for estimating exposure and risk to heat extremes in cities due to climate change.



529
 530 Fig. 8: Regions with high future exposure under climate change. E.g. Western Europe
 531 (region 1), the eastern USA (region 2), eastern China (region 3), western Africa (region
 532 4) and northern India (region 5), may face more risk in heat extremes coupled with the
 533 effect of urban heat islands in intensely urbanized places.

534 **5 Conclusions**

535 This study generated four key findings. First, the regions with the highest population
536 and GDP exposures to extreme heat are primarily concentrated in densely populated
537 areas, such as India, China, midwestern Europe, the eastern USA, and the coastal areas
538 of South America. Second, global population exposure for the years 2046–2065 is
539 highest under the RCP8.5-SSP3 scenario, with exposure increasing 3.76-fold relative
540 to the base period 1986–2005. The RCP2.6-SSP1 scenario produces the highest global
541 GDP exposure, with exposure increasing 10.47-fold for 2046–2065. Third, exposure is
542 highest for Asia for both population and GDP, which exceeds 50% of the global
543 exposure. The increase in exposure is largest for Africa, with the annual population and
544 GDP exposures 9.20- and 29.34-fold higher, respectively, than during the base period.
545 In contrast, the relative changes in population and GDP exposures are lowest for Europe
546 and North America, respectively. Fourth, the effect of climate is the dominant
547 contribution globally to change in population exposure, accounting for nearly half of
548 the total change (47%–53%). The effect of GDP is responsible for nearly 50% of the
549 total change in GDP exposure for 2016–2035, whereas the interactive effect makes the
550 primary contribution for 2046–2065 under the RCP4.5-SSP2 and RCP8.5-SSP3
551 scenarios, accounting for 49% and 53% of the total change, respectively. In conclusion,
552 mitigating emissions of greenhouse gases, either at the level of the RCP2.6 scenario or
553 at a more ambitious target of reduction, is important for reducing socioeconomic
554 exposure to heat extremes. In addition, designing and implementing effective measures
555 of adaptation are urgently needed in Asia and Africa to aid socioeconomic systems
556 suffering from heat extremes due to climate change.

557 **Acknowledgments**

558 This study was supported by the National Key Research and Development Program of
559 China (Grant No. 2016YFA0602402); the Youth Innovation Promotion Association,
560 CAS (Grant No. 2016049); the Program for “Kezhen” Excellent Talents in Institute of
561 Geographic Sciences and Natural Resources Research (IGSNRR), CAS, (Grant No.
562 2017RC101); the Key Research Program of Frontier Sciences, CAS (Grant No.
563 QYZDB-SSW-DQC005); and the ERC-SyG-2013-610028 IMBALANCE-P. We also
564 thank ISI-MIP and NIES for data support.

565 **References**

- 566 Barnett, A. G., Tong, S. & Clements, A. C. A., 2012. What measure of temperature is
567 the best predictor of mortality? *Environ. Res.* 118, 149–151.
568 <https://doi.org/10.1016/j.envres.2010.05.006>
- 569 Bonan, G. B., & Doney, S. C., 2018. Climate, ecosystems, and planetary futures: The
570 challenge to predict life in Earth system models. *Science*, 359(6375), eaam8328.
571 doi:10.1126/science.aam8328
- 572 Bouwer, L. M., 2013. Projections of future extreme weather losses under changes in

573 climate and exposure. *Risk Anal.* 33, 915–930. <https://doi.org/10.1111/j.1539->
574 6924.2012.01880.x

575 Bowles, D. C., Butler, C. D. & Friel, S., 2014. Climate change and health in Earth's
576 future. *Earths Future* 2, 60–67. <https://doi.org/10.1002/2013EF000177>

577 Burke, M., Hsiang, S. M. & Miguel, E., 2015. Global non-linear effect of temperature
578 on economic production. *Nature* 527, 235–239.
579 <https://doi.org/10.1038/nature15725>

580 Carleton, T. A. & Hsiang, S. M., 2016. Social and economic impacts of climate. *Science*
581 353, aad9837–aad9837. 10.1126/science.aad9837.
582 <https://doi.org/10.1002/2014GL061859>

583 Ceola, S., Laio, F. & Montanari, A., 2015. Satellite nighttime lights reveal increasing
584 human exposure to floods worldwide. *Geophys. Res. Lett.* 41, 7184–7190.
585 <https://doi.org/10.1002/2014GL061859>

586 Chen, J., Liu, Y., Pan, T., Liu, Y., Sun, F., & Ge, Q., 2018. Population exposure to
587 droughts in China under the 1.5° C global warming target. *Earth Syst Dynam*,
588 9(3): 1097-1106. <https://doi.org/10.5194/esd-9-1097-2018>.

589 Chen, L. & Frauenfeld, O. W., 2016. Impacts of urbanization on future climate in China.
590 *Clim dynam* 47, 345–357. <https://doi.org/10.1007/s00382-015-2840-6>

591 Cook, B. I., Smerdon, J. E., Seager, R. & Coats, S., 2014. Global warming and 21st
592 century drying. *Clim. Dyn.* 43, 2607–2627. <https://doi.org/10.1007/s00382->
593 014-2075-y

594 Dan, L. & Bou-Zeid, E., 2013. Synergistic Interactions between Urban Heat Islands and
595 Heat Waves: the Impact in Cities is Larger than the Sum of its Parts. *J Appl*
596 *Meteorol Clim* 52, 2051–2064. <https://doi.org/10.1175/JAMC-D-13-02.1>

597 Field, C. B., Barros, V. & Stocker, T. F., 2012. Managing the risks of extreme events
598 and disasters to advance climate change adaptation. Special report of the
599 Intergovernmental Panel on Climate Change (IPCC). Cambridge University
600 Press.

601 Fischer, E. M. & Knutti, R., 2015. Anthropogenic contribution to global occurrence of
602 heavy-precipitation and high-temperature extremes. *Nat. Clim. Change* 5, 560–
603 564. <https://doi.org/10.1038/nclimate2617>

604 Fischer, E. M., Oleson, K. W. & Lawrence, D. M., 2012. Contrasting urban and rural
605 heat stress responses to climate change. *Geophys res lett* 39, L03705.
606 <https://doi.org/10.1029/2011GL050576>

607 Forzieri, G., Cescatti, A., Silva, F. B. E. & Feyen, L., 2017. Increasing risk over time
608 of weather-related hazards to the European population: a data-driven prognostic
609 study. *Lancet Planet Health* 1, e200–e208. <https://doi.org/10.1016/S2542->
610 5196(17)30082-7

611 Garssen, J., Harmsen, C. & De, B. J., 2005. The effect of the summer 2003 heat wave
612 on mortality in the Netherlands. *Euro. Surveill.* 10, 165–168.
613 <https://doi.org/10.2807/esm.10.07.00557-en>

614 Gasparrini, A. & Armstrong, B., 2011. The impact of heat waves on mortality.
615 *Epidemiology* 22, 68–73. <https://doi.org/10.1097/ede.0b013e3181fdcd99>

616 Gasparrini, A. et al., 2015. Mortality risk attributable to high and low ambient

617 temperature: a multicountry observational study. *Lancet* 386, 369–375.
618 [https://doi.org/10.1016/S0140-6736\(14\)62114-0](https://doi.org/10.1016/S0140-6736(14)62114-0)

619 Grossman-Clarke, S., Zehnder, J. A., Loridan, T. & Grimmond, C. S. B., 2010.
620 Contribution of land use changes to near-surface air temperatures during recent
621 summer extreme heat events in the Phoenix metropolitan area. *J Appl Meteorol
622 Clim* 49, 1649–1664. <https://doi.org/10.1175/2010jamec2362.1>

623 Hajat, S. & Kosatky, T., 2010. Heat-related mortality: a review and exploration of
624 heterogeneity. *J Epidemiol Commun H* 64, 753–760.
625 <https://doi.org/10.1136/jech.2009.087999>

626 Harrington, L. J. & Otto, F. E. L., 2018. Changing population dynamics and uneven
627 temperature emergence combine to exacerbate regional exposure to heat
628 extremes under 1.5 °C and 2 °C of warming. *Environ. Res. Lett.* 13, 034011.
629 <https://doi.org/10.1088/1748-9326/aaaa99>

630 Hempel, S., Frieler, K., Warszawski, L., Schewe, J. & Piontek, F., 2013. A trend-
631 preserving bias correction - the ISI-MIP approach. *Earth Syst Dynam* 4, 219–
632 236. <https://doi.org/10.5194/esd-4-219-2013>

633 Hirabayashi, Y. et al., 2013. Global flood risk under climate change. *Nat. Clim. Change*
634 3, 816–821. <https://doi.org/10.1038/nclimate1911>

635 Hsiang, S. et al., 2017. Estimating economic damage from climate change in the United
636 States. *Science* 356, 1362–1369. <https://doi.org/10.1126/science.aal4369>

637 Huang, J. et al., 2017. Analysis of future drought characteristics in China using the
638 regional climate model CCLM. *Clim. Dyn.*, 50, 507–525.
639 <https://doi.org/10.1007/s00382-017-3623-z>

640 IPCC, 2013. *Climate Change 2013: The Physical Science Basis. Contribution of*
641 *Working Group I to the Fifth Assessment Report of the Intergovernmental Panel*
642 *on Climate Change.* Cambridge, UK, New York, USA: Cambridge University
643 Press.

644 IPCC, 2014. *Climate Change 2014: Impacts, Adaptation, and Vulnerability. Part A:*
645 *Global and 248 Sectoral Aspects. Contribution of Working Group II to the Fifth*
646 *Assessment Report of the 249 Intergovernmental Panel on Climate Change.*
647 Cambridge, UK, New York, USA: Cambridge University Press.

648 Jones, B. & O'Neill, B. C., 2016. Spatially explicit global population scenarios
649 consistent with the Shared Socioeconomic Pathways. *Environ. Res. Lett.* 11,
650 084003 (2016). <https://doi.org/10.1088/1748-9326/11/8/084003>

651 Jones, B., O'Neill, B.C., Mcdaniel, L., Mcginnis, S., Mearns, L.O. & Tebaldi, C., 2015.
652 Future population exposure to US heat extremes. *Nat. Clim. Change* 5, 592–
653 597. <https://doi.org/10.1038/nclimate2631>

654 Kharin, V. V., Zwiers, F. W., Zhang, X. & Wehner, M., 2013. Changes in temperature
655 and precipitation extremes in the CMIP5 ensemble. *Clim. Change* 119, 345–
656 357. <https://doi.org/10.1007/s10584-013-0705-8>

657 King, A. D., Karoly, D. J. & Henley, B. J., 2017. Australian climate extremes at 1.5° C
658 and 2° C of global warming. *Nat. Clim. Change* 7, 412–416.
659 <https://doi.org/10.1038/nclimate3296>

660 Liu, Z., Anderson, B., Yan, K., Dong, W., Liao, H. & Shi, P., 2017. Global and regional

661 changes in exposure to extreme heat and the relative contributions of climate
662 and population change. *Scientific Reports* 7, 43909.
663 <https://doi.org/10.1038/srep43909>

664 Maurer, E. P., 2007. Uncertainty in hydrologic impacts of climate change in the Sierra
665 Nevada, California, under two emissions scenarios. *Clim. Change* 82, 309–325.
666 <https://doi.org/10.1007/s10584-006-9180-9>

667 Mishra, V., Ganguly, A. R., Nijssen, B. & Lettenmaier, D. P., 2015. Changes in observed
668 climate extremes in global urban areas. *Environ Res Lett* 10, 024005.
669 <https://doi.org/10.1088/1748-9326/10/2/024005>

670 Mishra, V., Mukherjee, S., Kumar, R. & Stone, D. A., 2017. Heat wave exposure in
671 India in current, 1.5 °C, and 2.0 °C worlds. *Environ. Res. Lett.* 12, 124012.
672 <https://doi.org/10.1088/1748-9326/aa9388>

673 Mora, C. et al., 2017. Global risk of deadly heat. *Nat. Clim. Change* 7, 501–506.
674 <https://doi.org/10.1038/nclimate3322>

675 Murakami, D. & Yamagata, Y., 2016. Estimation of gridded population and GDP
676 scenarios with spatially explicit statistical downscaling, available at:
677 <https://arxiv.org/abs/1610.09041>.

678 Nath, R. et al., 2017. CMIP5 multimodel projections of extreme weather events in the
679 humid subtropical Gangetic Plain region of India. *Earths Future* 5, 224–239.
680 <https://doi.org/10.1002/2016EF000482>

681 O'Neill, B. C. et al., 2014. A new scenario framework for climate change research: the
682 concept of shared socioeconomic pathways. *Clim. Change* 122, 401–414.
683 <https://doi.org/10.1007/s10584-013-0905-2>

684 Oleson, K., 2012. Contrasts between urban and rural climate in CCSM4 CMIP5 climate
685 change scenarios. *J Clim* 25, 1390–1412. <https://doi.org/10.1175/JCLI-D-11-00098.1>

686

687 Riahi K et al., 2017. The shared socioeconomic pathways and their energy, land use,
688 and greenhouse gas emissions implications: an overview. *Glob Environ Change*
689 42:153-168. <https://doi.org/10.1016/j.gloenvcha.2016.05.009>

690 Robine, J. M., Cheung, S. L. K., Roy, S. L., Oyen, H.V., Griffiths, C., Michel, J. P. &
691 Herrmann, F. R., 2008. Death toll exceeded 70,000 in Europe during the summer
692 of 2003. *C. R. Biol.* 331, 171–178. <https://doi.org/10.1016/j.crv.2007.12.001>

693 Schlessner, C. F., Lissner, T. K., Fischer, E. M., Wohland, J., Perrette, M., Golly, A.,
694 Rogelj, J., CHILDERS, K., Schewe, J. & Frieler, K. 2016. Differential climate
695 impacts for policy-relevant limits to global warming: the case of 1.5 °C and 2 °C.
696 *Earth Syst Dynam*, 6, 2447–2505. <https://doi.org/10.5194/esd-7-327-2016>

697 Smirnov, O., Zhang, M., Xiao, T., Orbell, J., Lobben, A. & Gordon, J., 2016. The
698 relative importance of climate change and population growth for exposure to
699 future extreme droughts. *Clim. Change* 138, 1–13.
700 <https://doi.org/10.1007/s10584-016-1716-z>

701 Soden, B. J., Collins, W. D. & Feldman, D. R., 2018. Reducing uncertainties in climate
702 models. *Science* 361, 326–327. <https://doi.org/10.1126/science.aau1864>

703 Sun, H. et al., 2017. Exposure of population to droughts in the Haihe River Basin under
704 global warming of 1.5 and 2.0°C scenarios. *Quat. Int* 53, 74–84.

705 <https://doi.org/10.1016/j.quaint.2017.05.005>

706 Sun, Y. et al., 2014. Rapid increase in the risk of extreme summer heat in Eastern China.
707 Nat. Clim. Change 4, 1082–1085. <https://doi.org/10.1038/nclimate2410>

708 Taylor, K. E., Stouffer, R. J. & Meehl, G. A., 2012. An overview of CMIP5 and the
709 experiment design. Bull. Am. Meteorol. Soc. 93, 485–498.
710 <https://doi.org/10.1175/BAMS-D-11-00094.1>

711 Trenberth, K. E. & Fasullo, J. T., 2012. Climate extremes and climate change: The
712 Russian heat wave and other climate extremes of 2010. J. Geophys. Res. Atmos.
713 117, D17103. <https://doi.org/10.1029/2012JD018020>

714 UNFCCC Conference of the Parties (COP). 2015. Adoption of the Paris Agreement,
715 Paris, France.

716 Vaneckova, P., Beggs, P. J., de Dear, R. J. & Mccracken, K. W., 2008. Effect of
717 temperature on mortality during the six warmer months in Sydney, Australia,
718 between 1993 and 2004. Environ. Res. 108, 361–369.
719 <https://doi.org/10.1016/j.envres.2008.07.015>

720 Voorhees, A. S., Fann, N., Fulcher, C., Dolwick, P., Hubbell, B., Bierwagen, B. &
721 Morefield, P., 2011. Climate change-related temperature impacts on warm
722 season heat mortality: A proof-of-concept methodology using BenMAP.
723 Environ. Sci. Technol. 45, 1450–1457. <https://doi.org/10.1021/es102820y>

724 Vuuren, D. P. V. et al., 2011. The representative concentration pathways: an overview.
725 Clim. Change 109, 5–31. <https://doi.org/10.1007/s10584-011-0148-z>

726 Wang, J., Feng, J., Yan, Z., Hu, Y. & Jia, G., 2012. Nested high-resolution modeling of
727 the impact of urbanization on regional climate in three vast urban
728 agglomerations in China. J Geophys Res: Atmos 117, D21103.
729 <https://doi.org/10.1029/2012JD018226>

730 Wang, Y., Wang, A., Zhai, J., Tao, H., Jiang, T., Su, B., ... Fischer, T., 2019. Tens of
731 thousands additional deaths annually in cities of China between 1.5 °C and
732 2.0 °C warming. Nature Communications, 10(1), 3376.
733 <https://doi.org/10.1038/s41467-019-11283-w>

734 Warszawski, L., Frieler, K., Huber, V., Piontek, F., Serdeczny, O. & Schewe, J., 2014.
735 The inter-sectoral impact model intercomparison project (ISI-MIP): project
736 framework. Proc. Natl. Acad. Sci. U.S.A. 111, 3228–3232.
737 <https://doi.org/10.1073/pnas.1312330110>

738 Zhang, W., Zhou, T., Zou, L., Zhang, L., & Chen, X., 2018. Reduced exposure to
739 extreme precipitation from 0.5 °C less warming in global land monsoon regions.
740 Nature Communications, 9(1), 3153. <https://doi.org/10.1038/s41467-018-05633-3>

741

742 Zhang, Z., Li, N., Xu, H. & Chen, X., 2018. Analysis of the economic ripple effect of
743 the United States on the world due to future climate change. Earths Future 6,
744 828–840. <https://doi.org/10.1029/2018EF000839>